

MOLECULAR DYNAMICS STUDY ON THE FORMATION OF ORDERED ARRANGEMENT OF Ba-Ba ATOMIC PAIRS IN THE $\text{SiO}_2\text{-Al}_2\text{O}_3\text{-CaO-BaO}$ GLASS-CERAMIC

Fatih Ahmet ÇELİK¹ 

¹ Bitlis Eren University, Department of Physics, Turkey, facelik@beu.edu.tr

KEYWORDS

Glass-ceramic
Barium-Calcium aluminosilicate
Molecular dynamics
Born-Mayer-Huggins potential function

ARTICLE INFO

Research Article

DOI:

[10.17678/beuscitech.1335330](https://doi.org/10.17678/beuscitech.1335330)

Received 31 July 2023

Accepted 23 October 2023

Year 2023

Volume 13

Issue 2

Pages 159-169



ABSTRACT

In this study, the barium-calcium aluminosilicate ($\text{BaO-CaO-Al}_2\text{O}_3\text{-SiO}_2$) glass-ceramic system (BCAS) was modelled by using classical molecular dynamics (MD) simulation method based on Born-Mayer-Huggins (BMH) potential for interatomic interactions. The model system was heated to 5000 K and cooled to 300 K for obtaining a glassy structure. Then the temperature of the system was increased to 400 K, 500 K and 600 K temperatures for observing more ordered structure. For understanding of order formation, the structural development was analyzed by partial radial distribution function (PRDF). The results demonstrated that the PRDF peaks of Ba-Ba became sharper than other bond pairs with the increasing of annealing temperature. These sharp peaks at distant atomic distances represent the occurrence of ordered arrangement in Ba-Ba interactions.

1 INTRODUCTION

In recent years, new generation glass-ceramics have exhibited a number of remarkable physical characteristics when compared to the traditional ceramics and glasses [1-5]. Also, experimental studies have revealed the superior mechanical properties of these materials such as toughness, high flexural strength and fracture [6-8]. Therefore, they have a wide range of interesting technological and industry applications [9-12] because they are easily formed under different heat-treatment conditions via experimental methods [13-15]. At the end of these processes, these materials contain one or more embedded crystalline phases apart from remaining glass matrix. Recently, many studies have been carried out in different types of glass ceramics [16-20]. Among them, the XO-BaO-SiO₂-type glass ceramics (X = Mg, Zn and Ca) have attracted the attention for solid oxide fuel cell performance [21-23]. The Sr/BaO-Al₂O₃-SiO₂-B₂O₃-La₂O₃ systems have been investigated to understand how Ba/Sr content takes a role on coefficient of thermal expansion [1]. The effect of nucleating agents on glassy structure of XO-Al₂O₃-SiO₂-B₂O₃ glasses (R = Ba, Ca and Mg) have been investigated by Lahl et al. [24].

The several-type glass-ceramics have been fabricated for a variety of technological innovations. These studies show that one of the most important features expected from glass for glass-ceramic production is the ability to form suitable crystals without the need for long crystallization times [21-24]. Crystallization is facilitated when the network structure-modifying oxides are present in high amounts in the glass structure by adding CaO and BaO metal oxides. The addition of CaO and BaO to Al₂O₃-SiO₂ system causes various nucleation and crystallization processes [18, 21]. Therefore, the BaO- Al₂O₃-SiO₂ (BAS) glass ceramic materials have properties such as low thermal expansion and dielectric constant, high strength and corrosion resistance, and the CaO-Al₂O₃-SiO₂ (CAS) glass ceramic system is used in many industrial areas due to its good refractoriness, mechanical properties and optics [20-25]. In addition, barium-calcium aluminosilicate (BaO-CaO-Al₂O₃-SiO₂-BCAS) glass-ceramic appears to be very promise for use of chemical compatibility in a glass with metallic interconnects [26]. Specially, many researchers have focused on the BCAS systems by using experimental tools for fuel cell applications [1, 26].

Inspired by these experimental studies, we have also reported that the powerful computational methods are needed for understanding physical behaviors of these-type materials in the nanosized range [27]. The molecular dynamic (MD) simulation methods are a major tool for investigating the electronic, mechanical, optical, structural and phase transition processes of various materials at a nanoscale perspective [28-32]. However, in the literature, there are a few studies on the crystallization behaviors in nano-sized BCAS glass-ceramics under heat-treatment to detect the effect of XO addition on the structure of YO-SiO₂-Al₂O₃ system (X = Ba, Y = Ca, K, Mg).

In this study, the crystallization mechanism of BCAS glass-ceramic system have been investigated by using MD calculations based on the two-body BMH potential function. Its structural evaluation was carried out by radial distribution function (RDF) to understand the phase change mechanism during the annealing process.

2 MATERIALS AND METHODS

MD calculations are performed via SCIGRESS [34], a multiplatform molecular design, modeling and dynamics software. The potential energy function is selected as two-body BMH potential in Eq. 1 [35-37].

$$U_{ij}(r) = \frac{q_i q_j}{r_{ij}} + A_{ij} \exp(-B_{ij}r) - \frac{c_{ij}}{r_{ij}^6} \quad (1)$$

Where, r_{ij} denotes the distance between i and j atoms, $U_{ij}(r)$ is the interatomic-pair potential; $q_i q_j / r_{ij}$ is the long-range and, $A_{ij} \exp(-B_{ij}r)$ represents the short-range repulsion interactions. The initial MD simulation box consisted of randomly distributed CaOwt%46-SiO₂wt%46-Al₂O₃wt%5-BaOwt3% which included 6000 total atoms and had a 2.854 g/cm³ density [33] applying periodic boundary conditions along with all three directions. The time-step has chosen to be 1 fs with the NVT ensemble and the Nosé-Hoover thermostat [38] have been used during the simulation. The system held initial temperature of 5000 K for 50 ps for mixing of the system, and then the system was cooled to 300 K within 60 ps. Finally, the temperature of the system increased from 300 K to 400, 500, 600 K and the temperature was maintained at these temperatures for 90 ps to obtain an equilibrium state. A schematic diagram of the variation of temperature and potential

energy with simulation time is shown in Figure 1. After the relaxation process of the system, the equilibrium state of the model system at 5000 K temperature continued about 110 ps and then, the system was annealed to different temperatures from 300K.

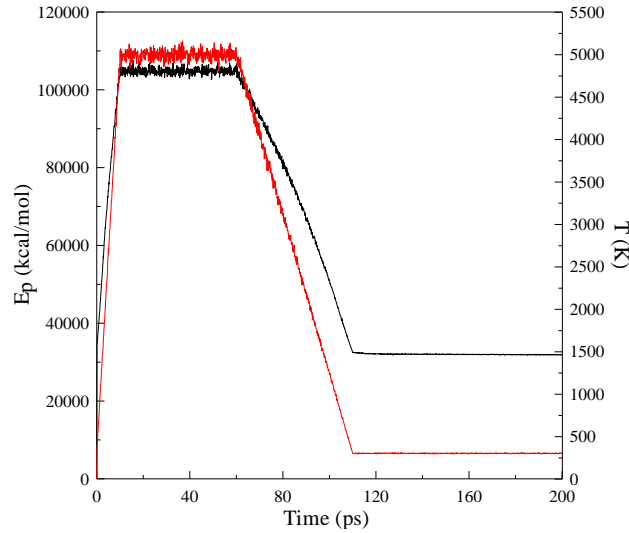


Figure 1. The schematic diagram of potential energy and temperature variation with simulation time.

3 RESULTS AND DISCUSSION

In MD simulations, RDF or $g(r)$ is one of the important structural analysis methods to examine the local order of a system during phase transition processes [39, 40]. The total RDF is defined as follows.

$$g(r) = \frac{V}{N^2} \left\langle \sum_{i=1}^n \frac{n(r)}{4\pi r^2 \Delta r} \right\rangle \quad (2)$$

where N represents the total number of atoms, V is the volume of the MD box, and $n(r)$ is the number of particles in the shell between r and $r+\Delta r$ [41]. Figure 2 shows the total RDF curves at 5000 and 300 K for BCAS system. At high temperature, the RDF curves exhibit broader than crystal structure, which is typical behavior characteristic of liquid. Also, the height of the first peak is less than that of glass or amorphous and crystal because there are very few atoms in the first neighborhood shell. At 300 K, the height of the first peak of RDF increases due to formation of the short-range clusters in the glass system. A minor splitting occurred in the second peak of RDF at 300 K upon the development of disordered structures in the second

neighborhood. Figure 3 shows the MD simulation result of the atomic positions of $\text{SiO}_2\text{-Al}_2\text{O}_3\text{-CaO-BaO}$ glass ceramic model system at 300 K.

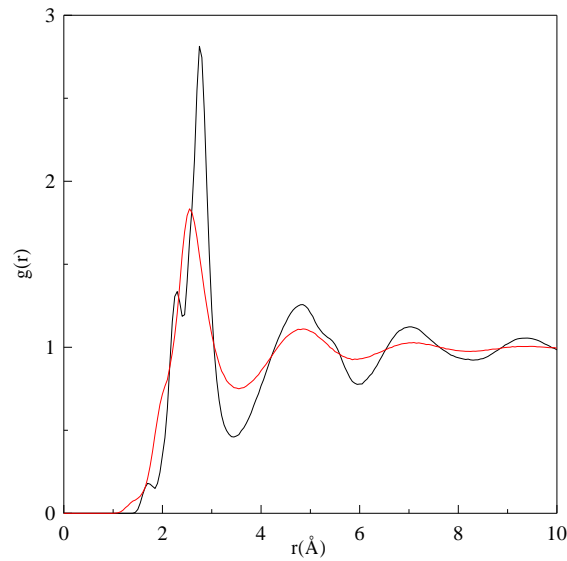


Figure 2. The total RDF curves for the system at 5000 K and 300 K temperatures (red lines represent 5000 K, black lines represent 300 K).

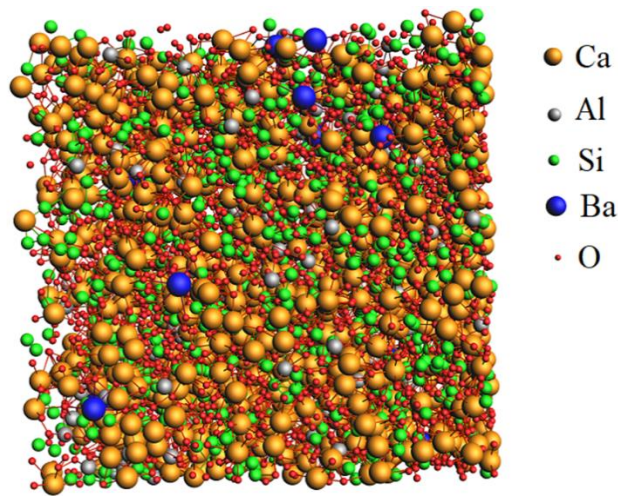


Figure 3. The simulation result of $\text{SiO}_2\text{-Al}_2\text{O}_3\text{-CaO-BaO}$ glass ceramic model system at 300 K (Al, Si, Ba, Ca, and O atoms are shown in grey, green, blue, yellow and red, respectively).

Some computed partial RDF's (PRDF) for BCAS system with different atomic bonded pairs at various annealing temperatures are shown in Figure 4 (a-b), Figure 5 (a-b), Figure 6 (a-b) and Figure 7 (a-b). As can be seen in these figures, we can be said that the PRDF curves exhibit a short-range order because there are no peaks at distant atomic positions [40] and they have strong first peak.

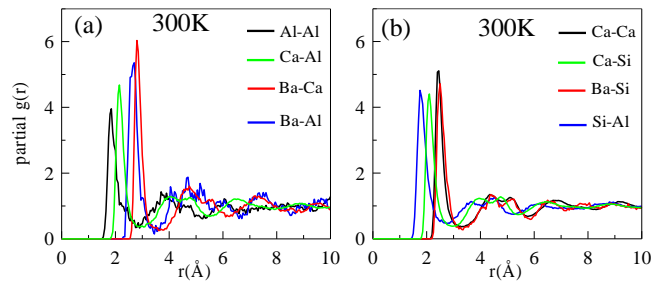


Figure 4. The PRDFs of atomic bonded pairs at 300 K annealing temperature a) Al-Al, Ca-Al, Ba-Ca and Ba-Al pairs b) Ca-Ca, Ca-Si, Ba-Si and Si-Al pairs.

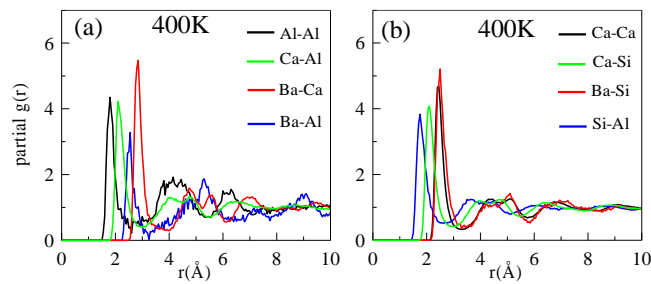


Figure 5. The PRDFs of atomic bonded pairs at 400 K annealing temperature a) Al-Al, Ca-Al, Ba-Ca and Ba-Al pairs b) Ca-Ca, Ca-Si, Ba-Si and Si-Al pairs.

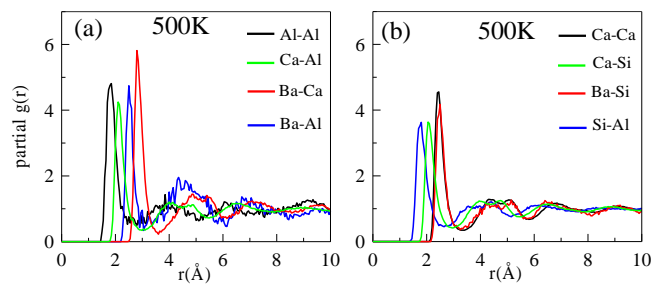


Figure 6. The PRDFs of atomic bonded pairs at 500 K annealing temperature a) Al-Al, Ca-Al, Ba-Ca and Ba-Al pairs b) Ca-Ca, Ca-Si, Ba-Si and Si-Al pairs.

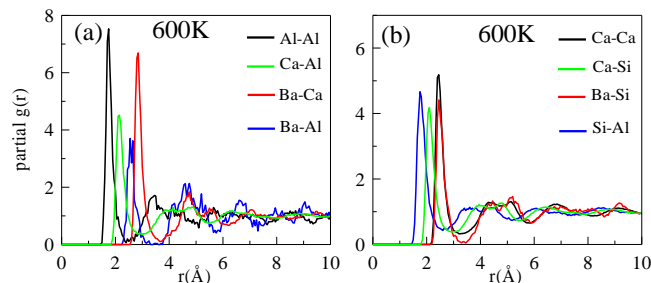


Figure 7. The PRDFs of atomic bonded pairs at 600 K annealing temperature a) Al-Al, Ca-Al, Ba-Ca and Ba-Al pairs b) Ca-Ca, Ca-Si, Ba-Si and Si-Al pairs.

Figure 8 shows the PRDFs of the bonded pairs in Ba-Ba interactions at various temperatures. The peaks in the PRDFs are sharper and have more distant atomic distances compared to the other bonded pairs. Especially, the height of the first peak of PRDF for Ba-Ba pairs is higher because the ordered periodic arrangement is dominant between Ba-Ba pairs array in the glassy structure. It was observed that the increasing of annealing temperature causes in better-defined ordered peaks for Ba-Ba interactions. From the position of the first peak in partial $g(r)_{\text{Ba-Ba}}$, it can be asserted that the Ba-Ba nearest-neighbor distances are calculated as 3.35 Å, 3.35 Å, 3.11 Å and 3.52 Å for 300 K, 400 K, 500 K and 600 K temperatures, respectively. This crystallization tendency between Ba-Ba atomic pairs can be explained with other studies on the BCAS glass ceramic. In recent years, a few studies have investigated how the content of Ba affects the crystallization behaviors of BCAS system. The addition of Ba to BCAS can decrease the viscosity of the mold flux [33]. The formation of ordered arrangements of Ba atoms can be reason behind this decrement in viscosity for BCAS system. Also, Bansal et al., [26] investigated the crystallization kinetics of a BCAS system by using experimental tools. They found that the crystallization activation energy of 259 kJ/mol for BCAS glass is much lower compared to other glass systems. This difference in activation energy have been evaluated as the silicate crystallization based on Ba which is formed firstly in BCAS glass different from other various glasses. In fact, the formation of this-type ordered array of Ba-Ba atomic pairs in a glass-ceramic has a complex microstructure with one or more crystalline phases [27]. Therefore, a basic modeling approach can help us close the gap between ordered formation observations in glassy structure in microscopic and macroscopic levels of materials.

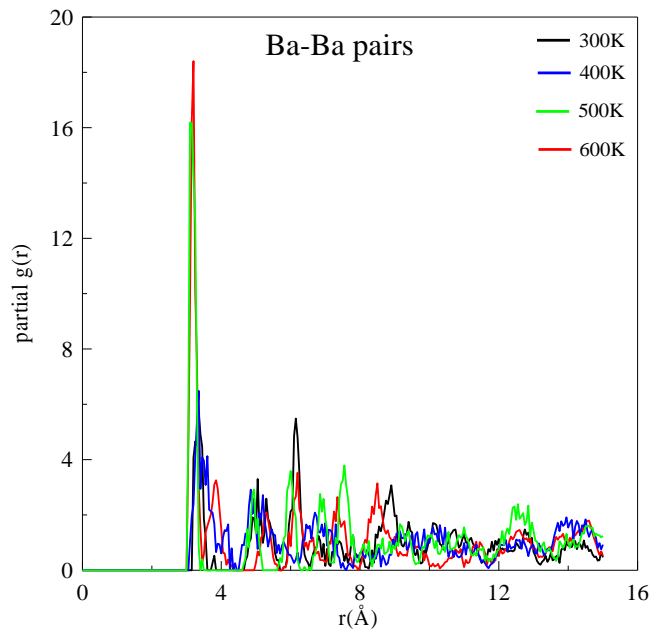


Figure 8. The variation of partial RDFs of Ba-Ba bonded pairs with annealing temperatures.

4 CONCLUSIONS

We conducted a classical molecular dynamics simulation on barium-calcium aluminosilicate ($\text{BaO-CaO-Al}_2\text{O}_3\text{-SiO}_2$) glass-ceramic system by using BMH potential function. The results of molecular dynamics indicated that while the height of the first peak of PRDF for Ba-Ba pairs was very sharp because of ordered structure between Ba-Ba pairs, the peak of the other pairs was not sharp because of glassy structure. The Ba-Ba nearest-neighbor distances were determined as 3.35 Å, 3.35 Å, 3.11 Å and 3.52 Å for 300 K, 400 K, 500 K and 600 K temperatures, respectively. The study is helpful in building up a modeling approach to understand the crystal formation behaviors in BCAS glass-ceramics at nanoscale.

Acknowledgment and support

This study was supported by the Bitlis Eren University Scientific Research coordination center (BEBAP Project number 2021.13). We grateful to BEBAP for the financial support of this work.

Statement of Research and Publication Ethics

The study is complied with research and publication ethics.

REFERENCES

- [1] S. Ghosh, A. D. Sharma, P. Kundu, S. Mahanty, and R. N. Basu, "Development and characterizations of BaO-CaO-Al₂O₃-SiO₂ glass-ceramic sealants for intermediate temperature solid oxide fuel cell application," *Journal of Non-Crystalline Solids*, vol. 354, no. 34, pp. 4081-4088, 2008.
- [2] R. Ota, N. Mishima, T. Wakasugi, and J. Fukunaga, "Nucleation of Li₂O- SiO₂ glass and its interpretation based on a new liquid model," *Journal of Non-Crystalline Solids*, vol. 219, pp. 70-74, 1997.
- [3] B. T. Hoa et al., "Structure, Morphology and Bioactivity of Bioactive Glasses SiO₂-CaO-P₂O₅ Doped with ZnO Synthesized by Green Synthesis," *Glass Physics and Chemistry*, vol. 48, no. 4, pp. 273-279, 2022.
- [4] R. D. Rawlings, J. P. Wu, and A. R. Boccaccini, "Glass-ceramics: their production from wastes—a review," *Journal of Materials Science*, vol. 41, pp. 733-761, 2006.
- [5] H. R. Fernandes et al., "Crystallization process and some properties of Li₂O-SiO₂ glass-ceramics doped with Al₂O₃ and K₂O," *Journal of the American Ceramic Society*, vol. 91, no. 11, pp. 3698-3703, 2008.
- [6] V. E. Pautkin, "Use of alkaline glass in micromechanical sensor structures," *Glass and Ceramics*, vol. 76, nos. 3-4, pp. 142-144, 2019.
- [7] H. Chen, T. Hong, and Y. Jing, "The mechanical, vibrational and thermodynamic properties of glass-ceramic lithium thiophosphates Li₄P₂S₆," *Journal of Alloys and Compounds*, vol. 819, 152950, 2020.
- [8] T. Sugawara et al., "Na₂O activity and thermodynamic mixing properties of SiO₂-Na₂O-CaO melt," *Journal of Non-Crystalline Solids*, vol. 371, pp. 58-65, 2013.
- [9] D. Herman, T. Okupski, and W. Walkowiak, "Wear resistance glass-ceramics with a gahnite phase obtained in CaO-MgO-ZnO-Al₂O₃-B₂O₃-SiO₂ system," *Journal of the European Ceramic Society*, vol. 31, no. 4, pp. 485-492, 2011.
- [10] H. Masai et al., "Surface crystallization of CaO-Bi₂O₃-B₂O₃-Al₂O₃-TiO₂ glass using IR furnace," *Journal of Non-Crystalline Solids*, vols. 356, nos. 52-54, pp. 2977-2979, 2010.
- [11] C. Thieme et al., "Effect of Al₂O₃ on phase formation and thermal expansion of a BaO-SrO-ZnO-SiO₂ glass ceramic," *Ceramics International*, vol. 44, no. 2, pp. 2098-2108, 2018.
- [12] K. El-Egili, "Infrared studies of Na₂O-B₂O₃-SiO₂ and Al₂O₃-Na₂O-B₂O₃-SiO₂ glasses," *Physica B: Condensed Matter*, vol. 325, pp. 340-348, 2003.
- [13] W. Zheng et al., "Effect of complex nucleation agents on preparation and crystallization of CaO-MgO-Al₂O₃-SiO₂ glass-ceramics for float process," *Journal of Non-Crystalline Solids*, vol. 450, pp. 6-11, 2016.
- [14] Q. C. Yu et al., "Effect of Fe₂O₃ on non-isothermal crystallization of CaO-MgO-Al₂O₃-SiO₂ glass," *Transactions of Nonferrous Metals Society of China*, vol. 25, no. 7, pp. 2279-2284, 2015
- [15] R. G. Duan, K. M. Liang, and S. R. Gu, "Effect of changing TiO₂ content on structure and crystallization of CaO-Al₂O₃-SiO₂ system glasses," *Journal of the European Ceramic Society*, vol. 18, no. 12, pp. 1729-1735, 1998.
- [16] C. Başaran et al., "The crystallization kinetics of the MgO-Al₂O₃-SiO₂-TiO₂ glass ceramics system produced from industrial waste," *Journal of Thermal Analysis and Calorimetry*, vol. 125, pp. 695-701, 2016.

- [17] S. C. Von Clausbruch et al., "The effect of P2O5 on the crystallization and microstructure of glass-ceramics in the SiO₂-Li₂O-K₂O-ZnO-P2O₅ system," *Journal of Non-Crystalline Solids*, vol. 263, pp. 388-394, 2000.
- [18] J. Partyka, "Effect of BaO ratio on the structure of glass-ceramic composite materials from the SiO₂-Al₂O₃-Na₂O-K₂O-CaO system," *Ceramics International*, vol. 41, no. 8, pp. 9337-9343, 2015.
- [19] E. Tkalcec, S. Kurajica, and H. Ivankovic, "Crystallization behavior and microstructure of powdered and bulk ZnO-Al₂O₃-SiO₂ glass-ceramics," *Journal of Non-Crystalline Solids*, vol. 351, nos. 2, pp. 149-157, 2005.
- [20] Z. E. Biskri et al., "Computational study of structural, elastic and electronic properties of lithium disilicate (Li₂Si₂O₅) glass-ceramic," *Journal of the Mechanical Behavior of Biomedical Materials*, vol. 32, pp. 345-350, 2014.
- [21] J. Kang et al., "Crystallization behavior and properties of CaO-MgO-Al₂O₃-SiO₂ glass-ceramics synthesized from granite wastes," *Journal of Non-Crystalline Solids*, vol. 457, pp. 111-115, 2017.
- [22] W. Zheng et al., "CaO-MgO-Al₂O₃-SiO₂ glass-ceramics from lithium porcelain clay tailings for new building materials," *Journal of Non-Crystalline Solids*, vol. 409, pp. 27-33, 2015.
- [23] X. Guo et al., "Crystallization and microstructure of CaO-MgO-Al₂O₃-SiO₂ glass-ceramics containing complex nucleation agents," *Journal of Non-Crystalline Solids*, vol. 405, pp. 63-67, 2014.
- [24] N. Lahl et al., "Crystallisation kinetics in AO-Al₂O₃-SiO₂-B₂O₃ glasses (A= Ba, Ca, Mg)," *Journal of Materials Science*, vol. 35, pp. 3089-3096, 2000.
- [25] Z. Yang et al., "Effect of CaO/SiO₂ ratio on the preparation and crystallization of glass-ceramics from copper slag," *Ceramics International*, vol. 40, no. 5, pp. 7297-7305, 2014.
- [26] N. P. Bansal and E. A. Gamble, "Crystallization kinetics of a solid oxide fuel cell seal glass by differential thermal analysis," *Journal of Power Sources*, vol. 147, nos. 1-2, pp. 107-115, 2005.
- [27] B. Deng et al., "Molecular dynamics simulations on fracture toughness of Al₂O₃-SiO₂ glass-ceramics," *Scripta Materialia*, vol. 162, pp. 277-280, 2019.
- [28] M. Celtek, S. Sengul, and U. Domekeli, "Glass formation and structural properties of Zr₅₀Cu_{50-x}Al_x bulk metallic glasses investigated by molecular dynamics simulations," *Intermetallics*, vol. 84, pp. 62-73, 2017.
- [29] S. Sengul, M. Celtek, and U. Domekeli, "Molecular dynamics simulations of glass formation and atomic structures in Zr₆₀Cu₂₀Fe₂₀ ternary bulk metallic alloy," *Vacuum*, vol. 136, pp. 20-27, 2017.
- [30] F. A. Celik and E. T. Korkmaz, "Molecular dynamic investigation of the effect of atomic polyhedrons on crystallization mechanism for Cu-based Cu-Pd and Cu-Pt alloys," *Journal of Molecular Liquids*, vol. 314, pp. 113636, 2020.
- [31] F. A. Celik, A. K. Yildiz, and S. Ozgen, "A molecular dynamics study to investigate the local atomic arrangements during martensitic phase transformations," *Molecular Simulation*, vol. 37, no. 05, pp. 421-429, 2011.
- [32] S. Kazanc, F. A. Celik, and S. Ozgen, "The investigation of solid-solid phase transformation at CuAlNi alloy using molecular dynamics simulation," *Journal of Physics and Chemistry of Solids*, vol. 74, no. 12, pp. 1836-1841, 2013.
- [33] Z. Piao et al., "Effect of BaO on the viscosity and structure of fluorine-free calcium silicate-based mold flux," *Journal of Non-Crystalline Solids*, vol. 542, pp. 120111, 2020.

- [34] SCIGRESS, Fujitsu Limited., Tokyo, Japan, 2021.
- [35] D. K. Belashchenko, "Computer simulation of the structure and properties of non-crystalline oxides," *Russian Chemical Reviews*, vol. 66, no. 9, pp. 733, 1997.
- [36] J. Kieffer and C. A. Angell, "Structural incompatibilities and liquid-liquid phase separation in molten binary silicates: A computer simulation," *The Journal of Chemical Physics*, vol. 90, no. 9, pp. 4982-4991, 1989.
- [37] K. Hirao and K. Kawamura, *Materials Design Using Personal Computer*, Shokabo, Tokyo, 1994, p. 52.
- [38] S. Nosé, "A unified formulation of the constant temperature molecular dynamics methods," *The Journal of Chemical Physics*, vol. 81, no. 1, pp. 511-519, 1984.
- [39] X. Li et al., "Tension-compression asymmetry of grain-boundary sliding: A molecular dynamics study," *Materials Letters*, vol. 325, 132822, 2022.
- [40] C. Li et al., "The concealed solid-solid structural phase transition of Fe₇₀Ni₁₀Cr₂₀ under high pressure," *Materials Today Communications*, vol. 33, 104499, 2022.
- [41] S. Özgen and E. Duruk, "Molecular dynamics simulation of solidification kinetics of aluminium using Sutton-Chen version of EAM," *Materials Letters*, vol. 58, no. 6, pp. 1071-1075, 2004.